ROCSCIENCE INTERNATIONAL CONFERENCE

THE EVOLUTION OF GEOTECH:
25 YEARS OF INNOVATION
APRIL 20–21, 2021

On the comparison of 2D and 3D stability analyses of an anisotropic slope

A. McQuillan
Rocscience, Inc.

N. Bar
Gecko Geotechnics

T. Yacoub
Rocscience, Inc.

RICAB108

This paper has been accepted and will be a part of the Rocscience International Conference 2021.

The paper will be published as a part of the conference proceedings by Taylor & Francis.

Taylor & Francis Group
an informa business

On the comparison of 2D and 3D stability analyses of an anisotropic slope

A. McQuillan[1], N. Bar[2] & T. Yacoub[1]
[1]*Rocscience, Inc.*

[2]*Gecko Geotechnics*

ABSTRACT: This paper summarizes the results of a parametric study that demonstrates the variability in Factor of Safety that is calculated for a highly bedded open pit mine when 2D and 3D limit equilibrium stability methods are applied. Factors of Safety are calculated for linear (Mohr-Coulomb) and non-linear (Generalized Hoek-Brown, Shear-Normal, Barton-Bandis) material models as well as different search settings. Results of this parametric study show that the Factor of Safety is consistently higher for 3D analysis, compared to 2D analysis. This increase in Factor of Safety, in this example, is attributed to the correct inclusion of end effects and varying directional strength, which is not possible to include in 2D analysis.

1 INTRODUCTION

Three-dimensional (3D) limit equilibrium (LE) modelling is increasingly being applied to assess the stability of open pit excavations. Previously, kinematic and two-dimensional (2D) LE modelling techniques were the most routinely applied to assess slope stability (Stacey 2007, McQuillan et al. 2019). However, as 3D LE software becomes more widely commercially available and more user friendly, geotechnical engineers are realizing the benefits of assessing stability in real world, three-dimensions (Bar et al. 2019a, Bar et al. 2019b, Bar et al. 2020. McQuillan et al. 2020).

3D stability analysis will always provide a more accurate representation of slope behavior and slope stability, especially where discontinuities strike more than 20 to 30º from the excavated face (Lorig and Varona 2007, Stacey 2007, Wines 2015, Cala et al. 2020). This is because the failure mechanism being modelled in 2D is always, at least to a degree, 3D in nature, so 2D analysis does not model the true mechanics of rock slope conditions and material strengths. For this reason, in many instances, material strengths derived from 2D back-analyses are higher than 3D-derived material strengths.

Variance in Factor of Safety (FOS) calculated between 2D and 3D methods will be more pronounced when the rock mass under investigation is anisotropic and/or the slope design includes confining geometries (Bar and Weekes 2017, Bar and McQuillan 2018). This is where 3D analysis can calculate a more realistic failure surface (e.g. model a slip surface that includes both sliding along bedding or foliation at the base of the slip surface and failure through rock mass bridges at all extremities of the slip surface – i.e. usually the toe, sides and crest).

Historically, 2D models were the most commonly constructed, due to their relative ease of model construction and rapid computation time (McQuillan et al. 2019). Sjoberg (1999) and Wines (2015) state that for relatively long open pits with basic geological conditions, 2D models can be justified. However, 2D LE analysis neglects the normal and horizontal side resisting forces along the sides of the sliding mass (i.e. end effects), which can lead to a conservative estimate of FOS (Shamsoddin Saeed et al. 2015). Neglect of this effect, or simply by applying a rule of thumb

adjustment to predict the 3D FOS equivalent, is a serious shortcoming of the current state of the art (Stacey 2007).

2D analyses also produce conservative indications of slope stability where worst-case scenarios are most often selected for 2D analysis. These worst-case scenarios will typically not be representative of all slope conditions (Sjoberg 1999, Duncan 2015, Wines 2015, Dana et al. 2018).

McQuillan et al. (2019) state that to reliably predict the performance (e.g. propensity for failure) and critical failure mechanism (including spatial location) of slope failure, geotechnical engineers must select appropriate tools to complete slope stability assessments. 3D LE is such a tool that can adequately account for the failure mechanisms typically observed in highly anisotropic geological settings.

This paper presents a parametric study that demonstrates the variability in FOS that is calculated for an anisotropic rock mass when 2D and 3D LE methods are applied. Sensitivity analysis are completed for linear and non-linear material models (e.g. Mohr-Coulomb, Generalized Hoek-Brown, Shear-Normal, Barton-Bandis) and slip surface search methods.

2 CASE STUDY

2.1 *Geological Setting*

An approximately 1280 m section of slope from a design in an iron ore mine has been used in this case study, Figure 1. The iron ore mine is located in the Pilbara region of Western Australia. This case study slope intersects the Newman formation, which displays anisotropic strength, with weaker strengths observed parallel and sub-parallel to bedding. Planar sliding along adversely orientated bedding planes and/or interbedded, weaker shale bands is the most common failure mechanism in the Pilbara region (Bar 2012, Seery 2015, Bar and Weekes 2017). Failures of this type occur at single bench to overall slope scale.

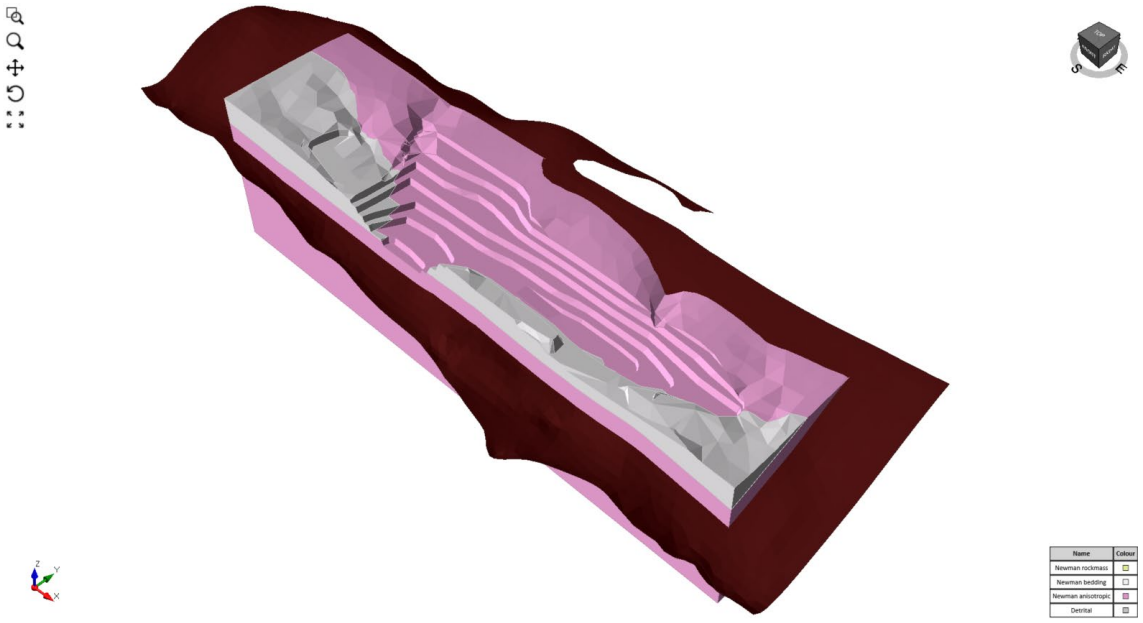

Figure 1 Parametric view of case study slope

2.2 *Parametric analysis*

To quantify the difference in FOS calculated using 2D and 3D LE methods, a series of models were computed with the following variables:

1. 3D models using the mine design, natural surface topography and lithological surfaces exported from the geological model (Figure 1). The deposit was above the

water table, so pore pressures were not considered. Anisotropy and true dip are included in 3D LE models;

2. 2D models using a 2D section cut through the middle of the critical FOS calculated from 3D modelling (Figure 2). Apparent dip is inherently included in 2D LE models;
3. 3D models derived by extruding the 2D section at varying lateral slope lengths (50 m, 100 m, 150 m, 200 m, 400 m). True anisotropy is not included in 2D extruded models. Instead, three dimensions are added by uniformly laterally extruding a 2D section;
4. Cuckoo vs Particle Swarm slip surface search methods, at varying search options (i.e. number of search surfaces and search depth limits); and
5. Linear (i.e. Mohr-Coulomb) and Non-Linear (Shear-Normal, Generalised Hoek-Brown and Barton Bandis) material strengths.

Rocscience, Inc.'s (2020) Slide2 (2D LE) and Slide3 (3D LE) software have been used to calculate the FOS of slope stability in this parametric study. Slide2 uses the method of slices, and Slide3 the method of columns, to sum the forces acting on the failure surface (i.e. mobilized stress) and compare these to the available shear strength.

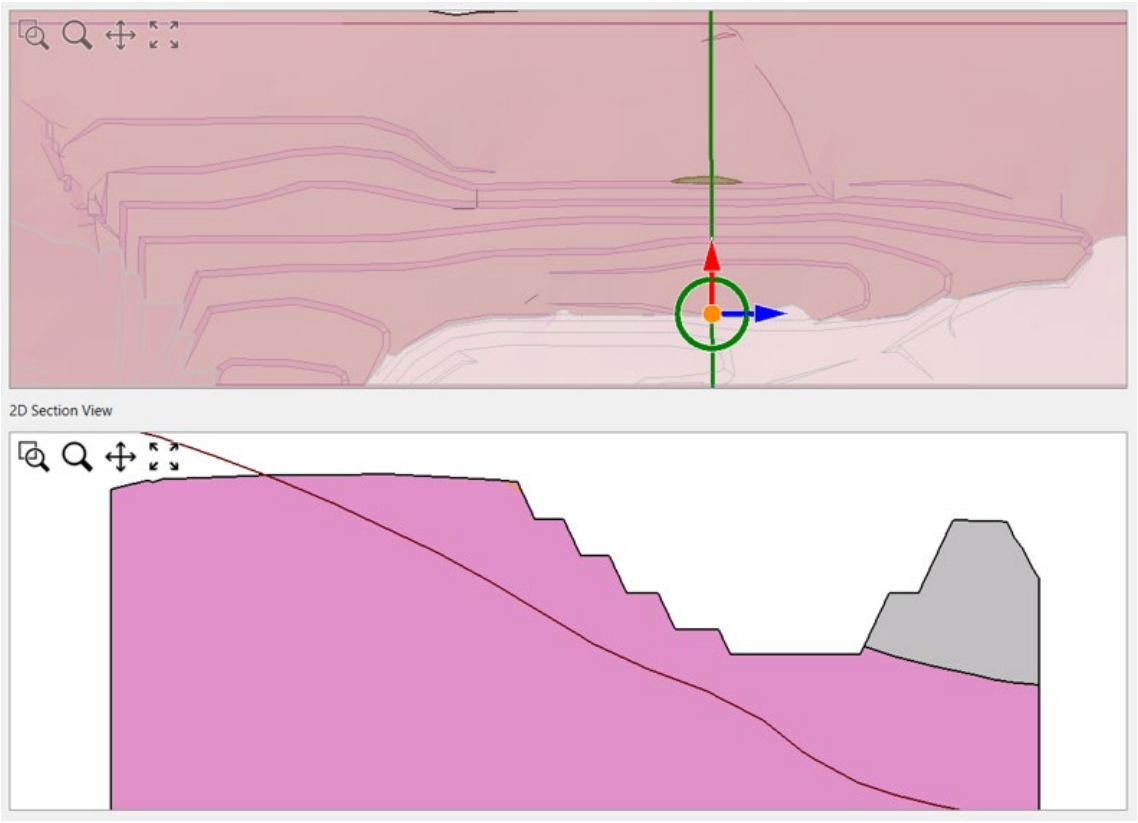

Figure 2 Plan view map showing location and cross-section cut for Slide2 analysis from the Slide3 model

Cuckoo and Particle Swarm are two metaheuristic search method algorithms built into Slide2 and Slide3 to search for the slip surface with the lowest FOS within the model search extents. Slide2 and Slide3 allows the user to vary the number of slip surfaces generated for each search method. The user can also define the minimum depth that slip surfaces are generated below the external boundary to test multi-bench stability. These options were enabled in the sensitivity analysis to determine the change in FOS calculated with: (i) varying search method; (ii) varying number of slip surfaces; and (iii) varying slip surface location to be able to simulate multi-bench slope failures.

Material strengths applied to LE models are summarized in Table 1 and Figure 3. Non-linear (Shear-Normal equivalents of Generalized Hoek-Brown and Barton-Bandis) material models were applied to LE models. Linear (Mohr-Coulomb) approximations of non-linear shear-strength envelopes were also applied to LE models to test the sensitivity of FOS to varying strength criteria. Linear material models have historically been applied to 2D LE models analyzing inter-ramp or overall slope failure so material models that cannot use non-linear shear strength inputs can be applied. However, non-linear material models are preferred, as their linear-equivalent approximations: (i) overestimate apparent cohesion and total shear strength at low normal stresses (e.g. ≤ 0.3 MPa); (ii) overestimate apparent friction and total shear strength at high normal stresses (e.g. ≥ 1.1 MPa); and (iii) underestimates shear strength at a normal stress of approximately 0.7 MPa (Bar and Weekes 2017), Figure 3.

Table 1 Modelled material strengths

Unit	Material Model	Model Parameters
Newman Shale – Bedding	Non-linear: Barton-Bandis (BB) and/or Shear-Normal	JRC = 2, JCS = 9, ϕ = 24 º
	Linear Approximation: Mohr-Coulomb (MC)	c = 9 kPa, ϕ = 26º
Weathered Newman Member – Rock mass	Non-linear: Generalised Hoek-Brown (GHB) and/or Shear-Normal	σ_c = 35 MPa, GSI = 40, mi = 10, D = 0.5
	Linear Approximation: Mohr-Coulomb	c = 210 kPa, ϕ = 44º

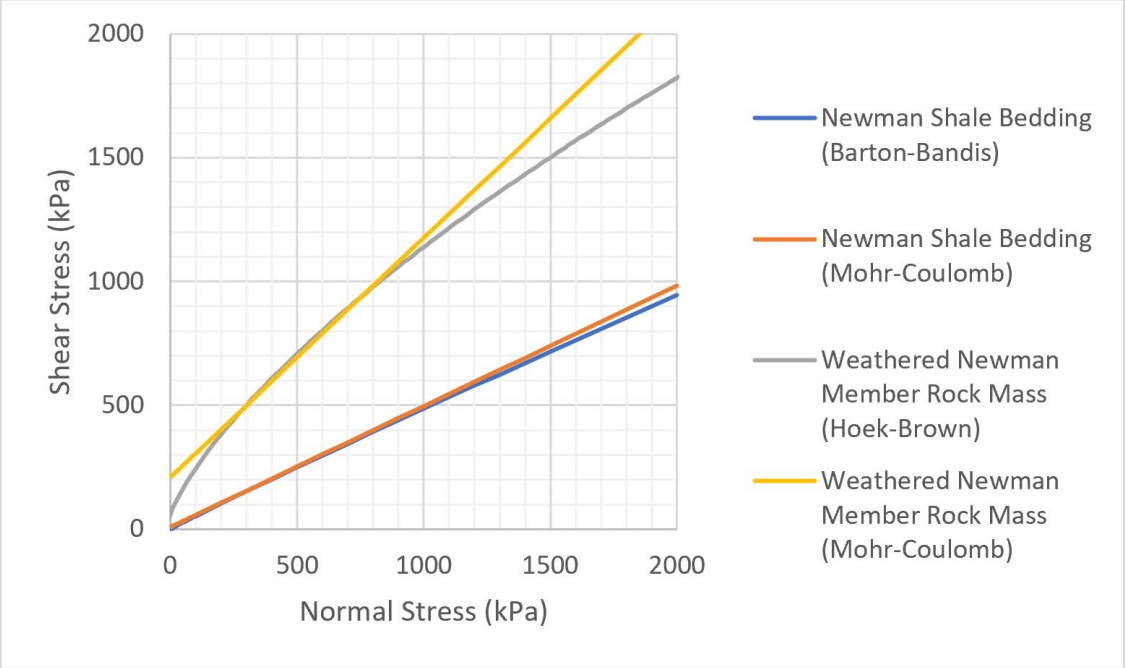

Figure 3 Graphical display of shear strengths applied to Newman Shale bedding and rock mass units

Anisotropy was included in 2D and 3D models using the Snowden Modified Anisotropic Linear (Mercer 2012, Mercer 2013) material model in Slide2 and Generalized Anisotropic material model in Slide3. These material models allow differential strengths for bedding and rock mass to be applied on the slip surface. A-values of 5º and B-values of 30º were applied in both 2D and 3D models, based on Bar and Weekes (2017).

2.3 *Results*

Parametric study results are summarized in Table 2 to Table 4, Figure 10 and Figure 12. FOS are reported for the GLE calculation method.

Table 2 Parametric study results – 3D LE analyses

Dimension	Material Model	Search Method	Number of Nests / Particles	Slope Depth Limit	Critical FOS_{GLE}	Reference Figure
3D	Non-linear (GHB + BB)	Cuckoo	20	None	0.90	Figure 4 A
		Cuckoo	80		0.89	Figure 4 B
		Particle Swarm	20		0.90	Figure 4 C
		Particle Swarm	80		0.81	Figure 4 D
3D	Non-linear (GHB + BB)	Cuckoo	20	15 m	1.13	Figure 5 A
		Cuckoo	80		1.00	Figure 5 B
		Particle Swarm	20		1.08	Figure 5 C
		Particle Swarm	80		1.06	Figure 5 D
3D	Linear (MC)	Cuckoo	20	None	1.10	Figure 6 A
		Cuckoo	80		1.11	Figure 6 B
		Particle Swarm	20		1.06	Figure 6 C
		Particle Swarm	80		1.11	Figure 6 D
3D	Linear (MC)	Cuckoo	20	15 m	1.12	Figure 7 A
		Cuckoo	80		1.10	Figure 7 B
		Particle Swarm	20		1.14	Figure 7 C
		Particle Swarm	80		1.09	Figure 7 D

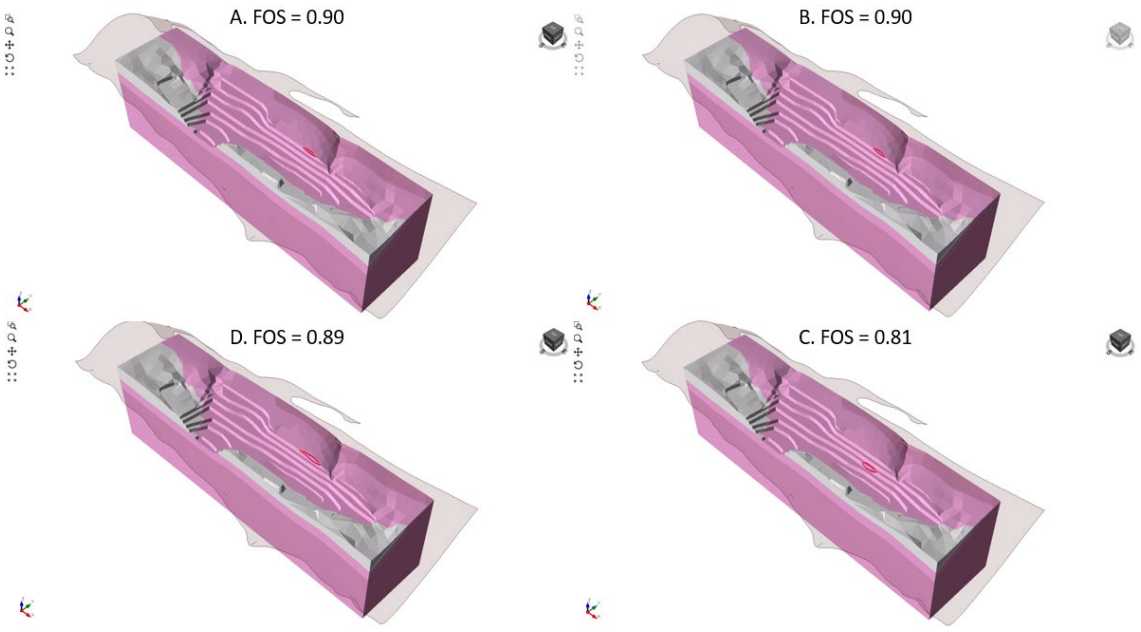

Figure 4 3D LE non-linear GLE FOS, unrestrained search limit

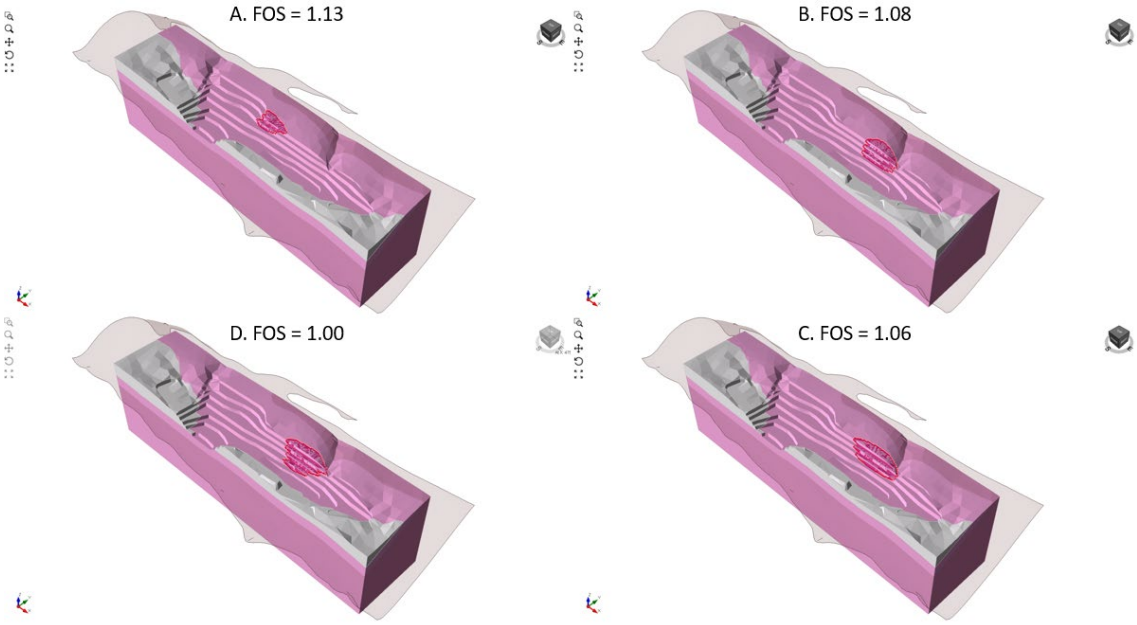

Figure 5 3D LE non-linear GLE FOS, 15 m depth search limit

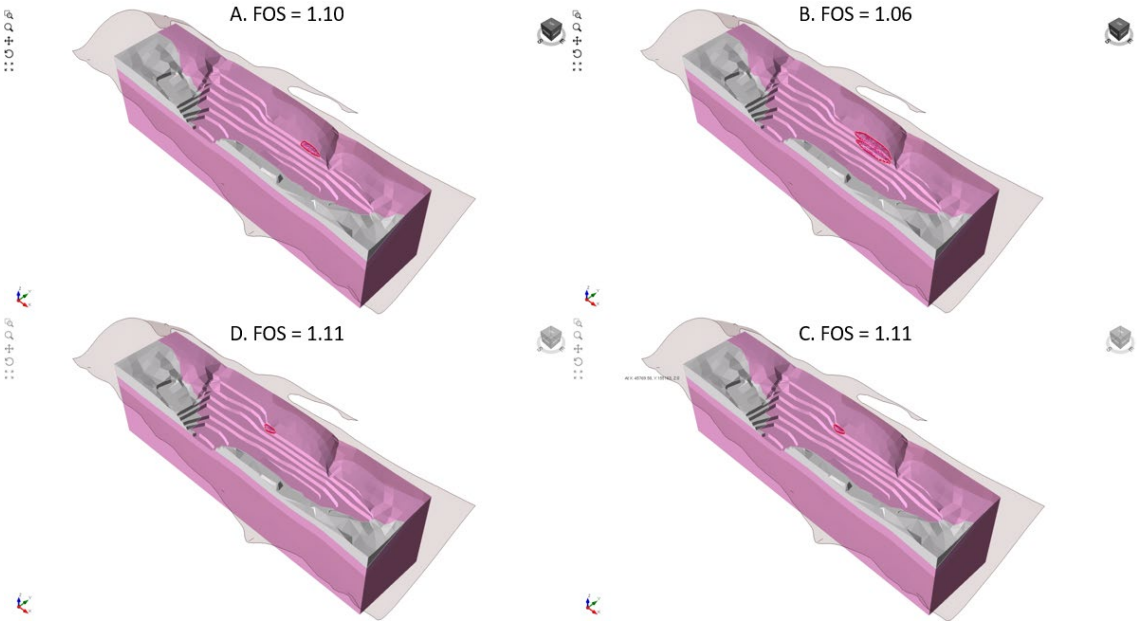

Figure 6 3D LE linear GLE FOS, unrestrained search limit

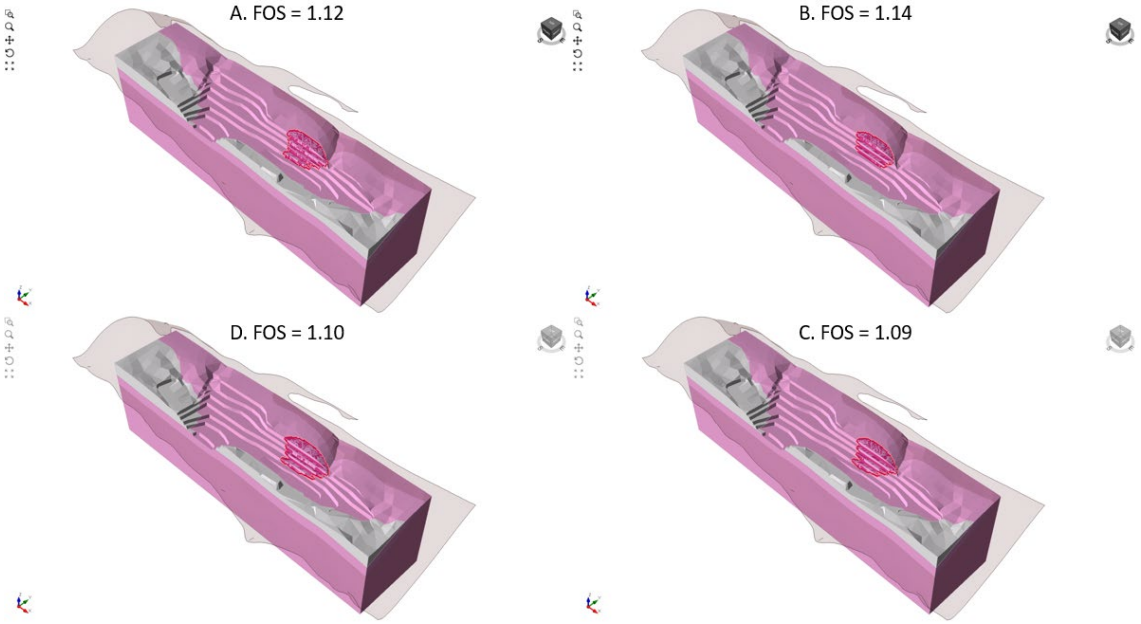

Figure 7 3D LE linear GLE FOS, 15 m depth search limit

Table 3 Parametric study results – 2D LE analyses

Dimension	Material Model	Search Method	Slope Depth Limit	Critical FOS_{GLE}	Reference Figure
2D	Non-linear (GHB + BB)	Cuckoo	None	0.73	Figure 8 A
		Particle Swarm		0.84	Figure 8 B
	Linear (MC)	Cuckoo		0.84	Figure 8 C
		Particle Swarm		0.88	Figure 8 D
2D	Non-linear (GHB + BB)	Cuckoo	15 m	0.80	Figure 9 A
		Particle Swarm		0.80	Figure 9 B
	Linear (MC)	Cuckoo		0.85	Figure 9 C
		Particle Swarm		0.85	Figure 9 D

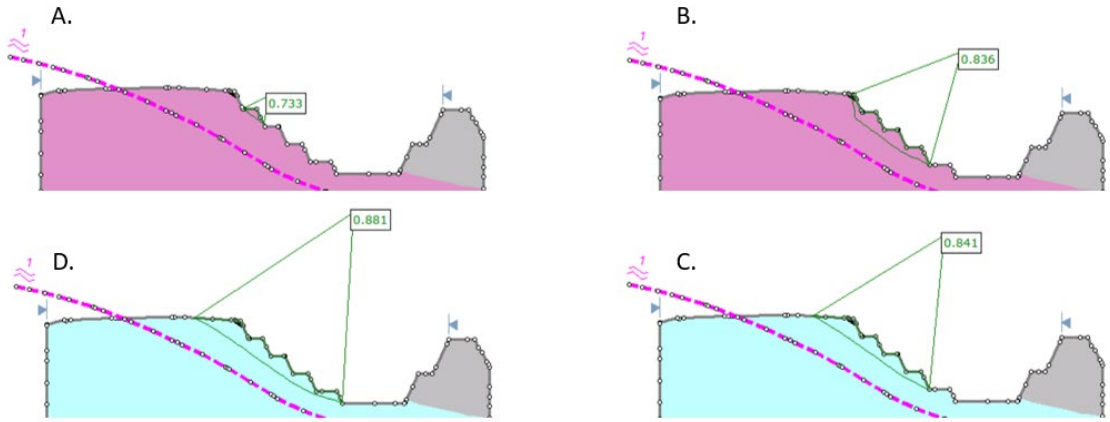

Figure 8 2D LE non-linear GLE FOS, unrestrained search limit

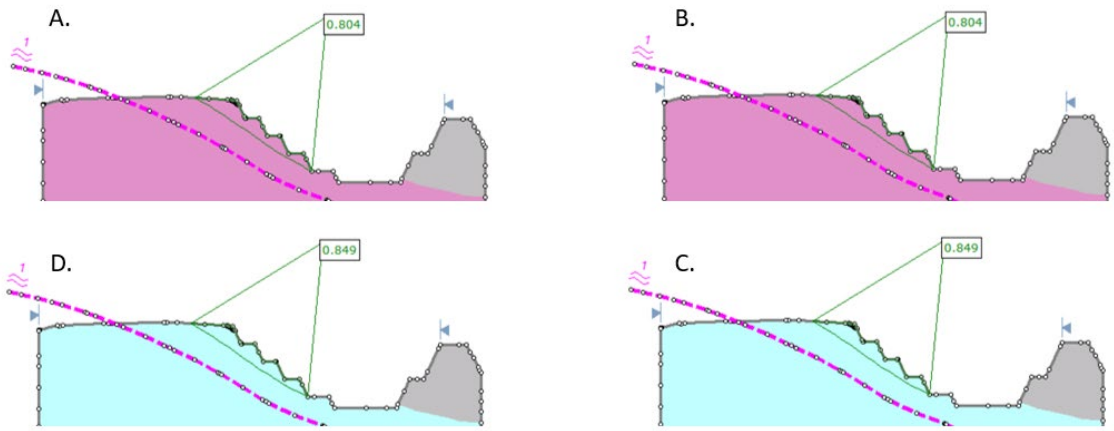

Figure 9 2D LE non-linear GLE FOS, 15 m search limit

Table 4 Parametric study results – 3D (2D extruded) LE analyses

Dimension	Material Model	Search Method	Slope Depth Limit	Number of Slip Surfaces	Critical FOS_{GLE}	Reference Figure
3D (extrusion length = 50 m)	Non-linear	Cuckoo	None	826	0.85	Figure 10
3D (extrusion length = 100 m)				1665	0.86	
3D (extrusion length = 200 m)				3288	0.85	
3D (extrusion length = 400 m)				6569	0.80	
3D (extrusion length = 50 m)	Non-linear	Cuckoo	15 m	845	1.15	Figure 10, Figure 11A
3D (extrusion length = 100 m)				1665	0.97	Figure 10, Figure 11B
3D (extrusion length = 200 m)				3306	0.97	Figure 10, Figure 11C
3D (extrusion length = 400 m)				6568	0.95	Figure 10, Figure 11D

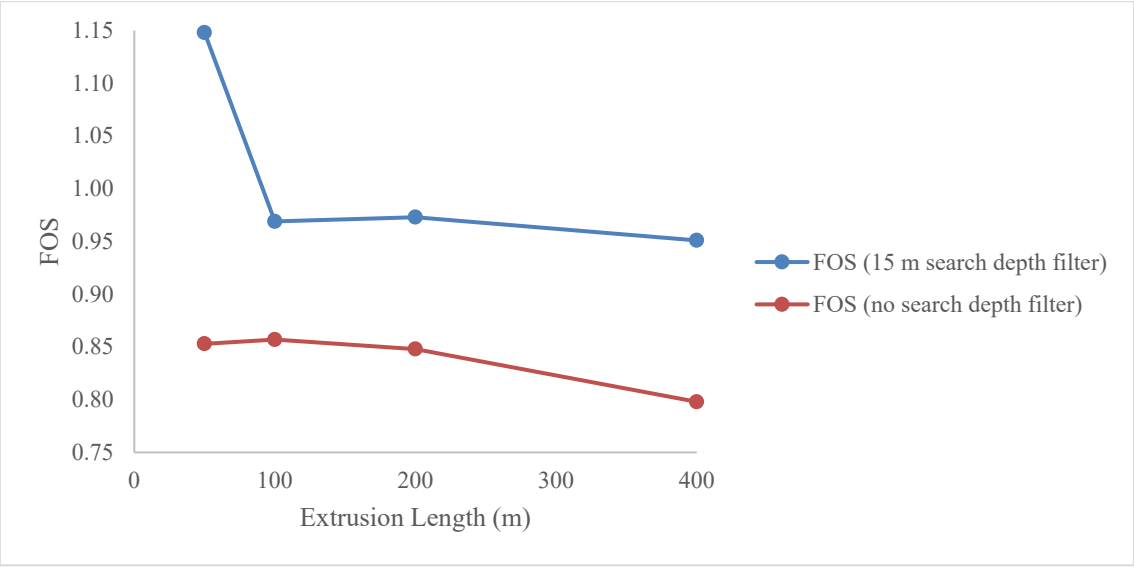

Figure 10 2D extruded non-linear GLE FOS

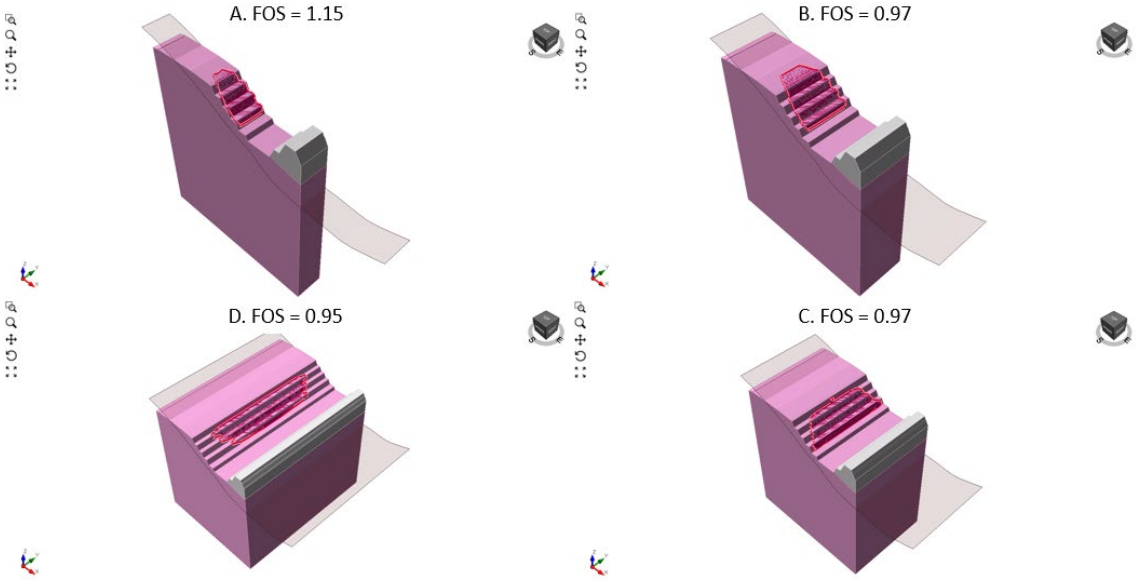

Figure 11 2D extruded FOS, 15 m depth search limit. Slip surfaces are constrained at edge of Slide3 model at 50 m, 100 m and 200 m extruded depths

3 DISCUSSION AND RECOMMENDATIONS

Sensitivity analyses of 2D and 3D search methods, non-linear and linear material models, search method, number of slip surfaces, and search limit depth of an anisotropic rock mass indicate the following:

Sensitivity analysis with different search methods and different numbers of slip surfaces should be completed to determine the critical FOS. The number of slip surfaces calculated should adequately cover the section of slope being analyzed. Default software settings may not produce an adequate number of slip surfaces in the search to find the critical FOS in the slope under investigation.

Non-linear material models generally result in a lower FOS being calculated, compared to linear material models. Previous publications by Bar and Weekes (2017) support these findings that non-linear material models are better suited to model anisotropic rock masses where shallow failures are expected along pitwards dipping structures.

Applying search depth limits provides an estimate of multi-bench stability, which generally have higher FOS compared to scenarios where no search depth limits are applied.

The length of 3D models, created from the extrusion of 2D sections, will impact the FOS calculated. The shorter the width (i.e. the more confined) the extruded model, the higher the FOS will be. Slip surfaces should be reviewed to ensure their extents are not constrained to the boundaries of the 3D model. If this is condition is observed, the critical FOS may not have been found.

The FOS calculated from 2D analyses are generally lower (average 25%) than the FOS calculated from 3D analysis. The difference in FOS is more pronounced in models with linear material models applied (average FOS 30% lower). In this parametric study the increase in 3D FOS is attributed to the inclusion of rock mass strength at the sides of the failure surface (i.e. end effects) in the anisotropic rock mass, Figure 12, Figure 13 and Figure 14. Such forces will not be included in 2D analyses.

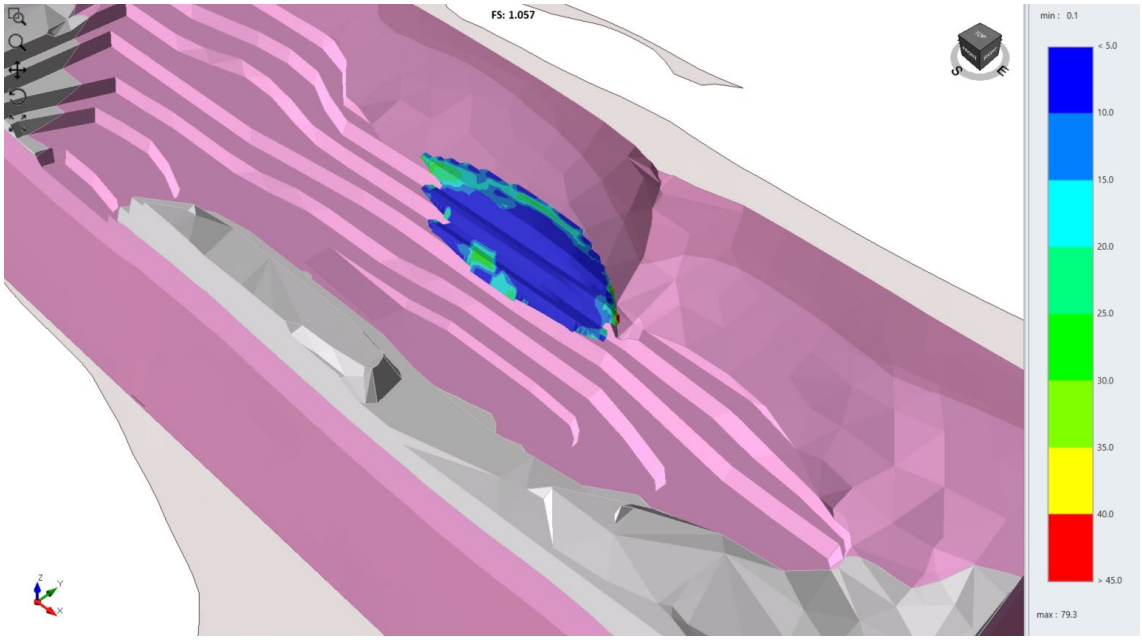

Figure 12 Perspective view of critical slip surface showing variation in cohesion applied to column bases relative to applied Generalised Anisotropic strength function

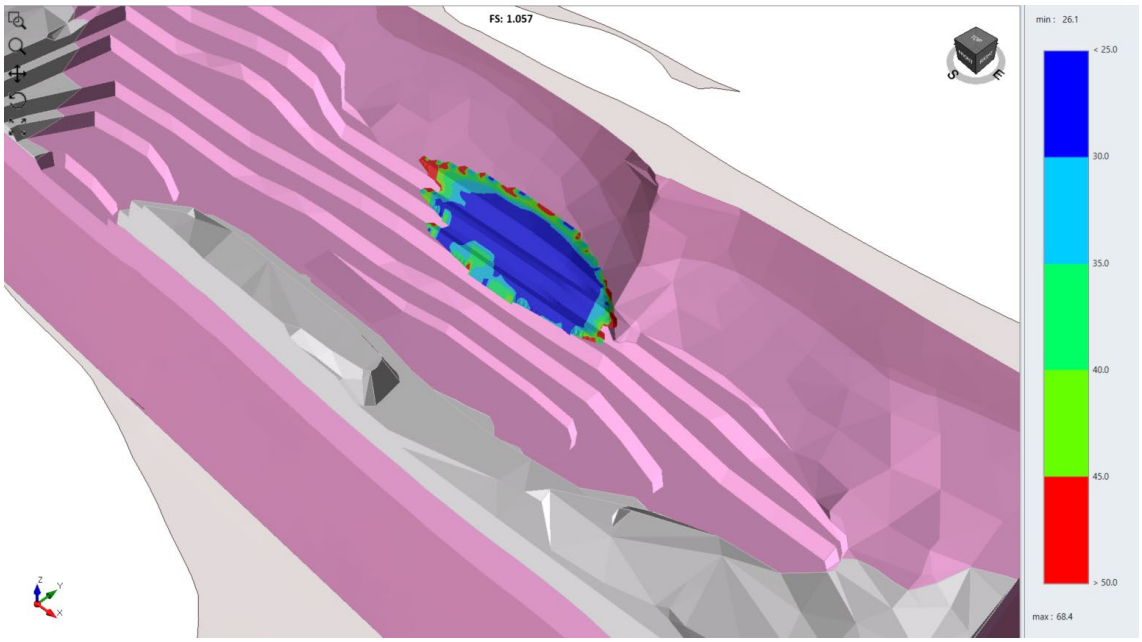

Figure 13 Perspective view of critical clip surface showing variation in friction angle applied to column bases relative to applied Generalised Anisotropic strength function

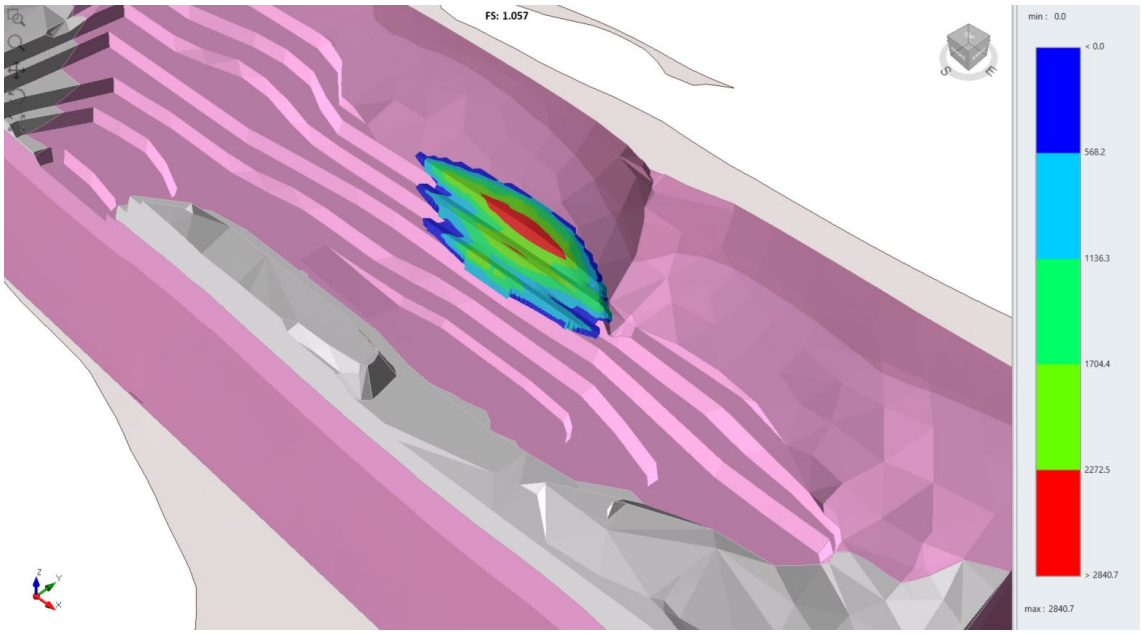

Figure 14 Perspective view of critical clip surface showing variation in base shear force along column bases

4 CONCLUSIONS

3D models allow geotechnical engineers to model the true ground conditions which are generally always anisotropic in nature. This paper has demonstrated the variance in FOS when calculated using 2D and 3D LE methods. The case study utilized in the parametric study has shown that for anisotropic rock masses, 3D LE consistently produces a higher FOS. This is expected where 3D analysis allows a more accurate representation of failure mechanism, as the slip surface that is created considers the strength of the sides of the slip surface, which are not considered in 2D analysis.

3D LE software is now widely commercially available. Such tools provide geotechnical engineers a means of rapidly predicting slope performance to assist in the risk management and slope optimisation open pit slope designs.

5 REFERENCES

Bar, N. 2012. Performance driven slope management, design and optimization at Brockman Operation, Rio Tinto Iron Ore. In Proceedings: 9th Young Geotechnical Professionals Conference (9YPGC), St Kilda, Australian Geomechanics Society, pp. 19-24.

Bar N, Weekes G. Directional shear strength models in 2D and 3D limit equilibrium analyses to assess the stability of anisotropic rock slopes in the Pilbara region of Western Australia. Australian Geomechanics Journal 2017; 52(4); 91-104.

Bar N, McQuillan A. 3D Limit Equilibrium Slope Stability Analysis for Anisotropic and Faulted Rock Masses in Australian Coal and Iron Ore Mines, In: Proc. ISRM International Symposium - ARMS10, Singapore, 2018; 12p.

Bar, N. Kostadinovski, M. Tucker, M. Byng, G. Rachmatullah, R. Maldonado, A. Pőtsch, M. Gaich, A. McQuillan, A. Yacoub, T. 2020. Rapid and robust slope failure appraisal using aerial photogrammetry and 3D slope stability models. International Journal of Mining Science and Technology. https://doi.org/10.1016/j.ijmst.2020.05.013

Bar N, Ryan C, Yacoub TE, McQuillan A, Coli N, Leoni L, Harries N, Rea SA, Bu J. Integration of 3D limit equilibrium models with live deformation monitoring from interferometric radar to identify and manage slope hazards. Proc. ISRM 14th International Congress of Rock Mechanics, Iguassu Falls, Brazil, 2019a.

Bar N, Yacoub TE, McQuillan A. Analysis of a large open pit mine in Western Australia using finite element and limit equilibrium methods. Proc. ARMA 2019: 53rd US Rock Mechanics / Geomechanics Symposium, New York, United States of America, 2019b.

Bromhead E. Landslide slip surfaces: their origins, behavior and geometry, Landslides: Evaluation and Stabilization 2004, Taylor & Francis Group, London.

Cala, M. Cyran, K. Kakóbczyk, J. Kowalski, M. 2020. The challenges of open pit mining in the vicinity of the salt dome (Bełchatów Lignit deposit, Poland). Energies. Vol. 13. doi:10.3390/en13081913

Cheng Y, Yip C. Three-dimensional asymmetrical slope stability analysis extension of Bishop's, Janbu's, and Morgenstern-Price's techniques. J. Geotech. Geoenviron. Eng 2007; 133(12); 1544-1555.

Dana, H. Kakaie, R. Rafiee, R. Bafghi, Y. 2018. Effects of geometrical and geomechanical properties on slope stability of open-pit mines using 2D and 3D finite difference methods. Journal of Mining & Environment. Voly. 9(4), pp. 941-957.

Duncan J. State of the art: Limit equilibrium and finite-element analysis of slopes. J. Geotech. Engng 1996; 122(7); 577-596.

Lorig L, Varona P. Numerical Analysis, Rock Slope Engineering, Civil and Mining, 4th Edition. C. Wyllie and C.W. Mah (eds). Spon Press; 2007.

Mercer, K. 2012. The history and development of the anisotropic linear model: part 1. Australian Centre for Geomechanics, Perth. Western Australia.

Mercer, K. 2013. The history and development of the anisotropic linear model: part 2. Australian Centre for Geomechanics, Perth. Western Australia.

McQuillan A, Canbulat I, Oh J. 2020. Methods applied in Australian industry to evaluate coal mine slope stability. International Journal of Mining Sciences and Technology. Vol 30(2), pp. 151-155. https://doi.org/10.1016/j.ijmst.2019.11.001

Seery, J. 2015. Limit equilibrium analysis of a planar sliding example in the Pilbara Region of Western Australia – comparison of modelling discrete structure to three anisotropic share strength models. In Proceedings: SAIMM Slope Stability 2015, Cape Town, pp. 681-696.

Shamsoddin Saeed, M. Maarefvand, P. Yaaghubi, E. 2015. Two and three-dimensional slope stability analyses of final wall for Miduk mine. International Journal of Geo-Engineering. DOI 10.1186/s40703-015-0009-0.

Sjoberg J. Analysis of Large Scale Rock Slopes, PhD Thesis, Lulea University of Technology Department of Civil and Mining Engineering Division of Rock Mechanics, Sweden; 1999.

Stacey, T. 2007. Slope stability in high stress and hard rock conditions. In Proceedings: International Symposium on Rock Slope Stability in Open Pit Mining and Civil Engineering (Slope Stability 2007). Perth, pp. 187-200.

Wines D. A comparison of slope stability analyses in two and three dimensions. In: Proc. SAIMM Slope Stability 2015, Cape Town, South Africa, 2015; 305-316.

Wines, D. A comparison of slope stability analyses in two and three dimensions. The Journal of the Southern African Institute of Mining and Metallurgy. Vol. 116, pp. 399-406.